APPLICATION OF THE DRIFT FLUX MODEL IN A TWO-PHASE REFRIGERANT FLOW THROUGH CAPILLARY TUBE

M.R. Barbosa, mariengquim@gmail.com
R.A. Mazza, mazza@fem.unicamp.br
State University of Campinas, Rua Mendeleyev 200, Campinas, 13083-860, Brazil

Abstract. *A drift flux model has been used to study the two-phase flow during vaporization of halogenated refrigerants (R12 and R134a) through an adiabatic capillary tube, which is employed as expansion devices in small sized refrigeration systems. The capillary tube has an internal diameter ranging from 0.66 to 1.17 mm and the inlet pressure varying from 0.8 to 1.4 MPa. The flow is considered as one-dimensional, stationary and thermodynamic equilibrium between liquid and vapor phases is assumed. The model applies a flow pattern independent void fraction correlation and was validated against experimental pressure drop data found in literature. The generation of vapor induce a flow pattern change, which is presented. A comparison of the results of drift flux and two-fluid model shows a good agreement to pressure distribution, void fraction, quality and phases velocities.*

Keywords*: drift-flux model; adiabatic flow; capillary tube; flow pattern map.*

1. NOMENCLATURE

A	Area, m²
c	Constant, kg/s
C_o	Distribution parameter
$C_{o,1}$	Parameter of drift flux model, dimensionless
C_2	Parameter of drift flux model, dimensionless
C_3	Parameter of drift flux model, dimensionless
C_f	Fanning friction factor, dimensionless
D	Diameter, m
F	Empirical flash coefficient, dimensionless
Fr	Froude number, dimensionless
G	Mass flux, kg/(m².s)
g	Acceleration due to gravity, m/s²
h	Enthalpy, J/kg
J	Superficial velocity, m/s
L	Capillary tube length, m
La	Laplace variable, dimensionless
P	Pressure, N/m²
R_B	Radius of a nucleation site, m
Re	Reynolds number, dimensionless
S	Perimeter, m
T	Temperature, K
U	Actual velocity, m/s
U_{Gm}	Drift velocity, m/s
We	Weber number, dimensionless
x	Quality, dimensionless
z	Axial length, m

Greek

α	Void fraction, dimensionless
Δ	Finite variation
ε	Tube wall roughness, m
μ	Dynamic viscosity, kg/(m.s)
ϖ	Implicit Runge-Kutta term, N/m²
ρ	Density, kg/m³
σ	Surface tension, N/m
τ	Shear stress, N/m²

Subscripts

G	Vapor phase
L	Liquid phase
M	Mixture
ms	Measured
sat	Saturated
nuc	Nucleation sites

2. INTRODUCTION

A capillary tube is a constant area expansion device with an internal diameter ranging from 0.5 to 2.0 mm and length between 1 and 6 m (Seixlack et al., 2014). It was developed for refrigeration equipment applications such as household refrigerators and small air conditioners, as well as gas expansion thermometers and connection lines for pneumatic control.

There are many advantages related to the usage of capillary tube instead of automatic expansion valve: reliability, low cost, absence of moving parts and capability to operate in reverse cycle. However, the main drawbacks are capillary clogging caused by moisture presence and impossibility of changing its characteristic dimensions when it is designed to a specific operational condition (Mezavila, 1995).

Various researches has reported the evaporation rate and fluid flow parameters (quality, velocity and void fraction) for two-phase flow of halogenated refrigerant fluid. Some data found in the literature were discussed by Wallis (1980), who divided the study into two categories: nonequilibrium and equilibrium flow. The first one considers the interphase heat, mass and momentum transfer. On the other hand, the last one assumes that the temperature and pressure are the same between the vapor and liquid in a tube section, so there is no heat transfer between the phases and the velocities could be determined by homogeneous or drift-flux model.

In the study of the refrigerant two-phase flow, some authors assume an entrance of a subcooled liquid in a capillary tube. Due to the friction, the pressure declines and reaches the saturation pressure at the inlet temperature. This is the

flash point and the liquid vaporization may begin. Lin et al., (1991) studied the pressure loss during the vaporization of R12 along the capillary and noticed a delay in the vaporization process due to saturated liquid surface tension and the imminent bubble, which prevents the phase vapor arising. The authors named it as metastable phenomenon and have associated it to a thermodynamic instability throughout the tube. After this point, the vibrations or the tube roughness allows the beginning of bubbles formation (Mezavila, 1995) and the phases velocities could be determined through a solution algorithm based on two-fluid model (Seixlack et al., 2014), or on drift-flux approach (Liang and Wong, 2001), or homogeneous flow (Ingle et al., 2015).

Experimental evidences show that the two-phase flow in capillary tubes is not entirely homogeneous, so the hypothesis of non-slip flow can wrongly estimate the pressure drop and the distribution of the phases. Besides, the use of the two-fluid model for capillary tube description is complex because this requires a large number of unknown closure relationships dependent on the flow pattern, such as: interfacial force and friction factor. As an alternative, some authors (Madsen, 1975; Chisholm, 1973) proposed a flow pattern independent expression for vertical and horizontal orientations based on Zuber and Findlay (1965) correlation. More recently, Bhagwat and Ghajar (2014) proposed a general void fraction equation using a wide range of two-phase fluid combination, hydraulic pipe diameter and pipe orientation database in order to estimate the parameters of the drift-flux model.

Although the void fraction estimated by Bhagwat and Ghajar (2004) is not dependent on flow pattern, it is necessary to know the phase distribution in order to elaborate efficient projects based on head loss, relative velocity, intermittency fraction and heat or mass transfer (Arcanjo et al., 2010). Very limited data are available for refrigerant flow pattern investigation, those are commonly determined from experimental observations and are limited to the conditions near those of the mass flow rate, quality and reduced temperature measurements. Yang and Shieh (2001) suggested a comparative study of flow maps for horizontal small channels ranging in diameter size from 1 mm to 3 mm, using R134a and air-water two-phase flow. The authors concluded that the surface tension force is one of the important parameters to define the pattern transitions.

This work compares the numerical results based on Bhagwat and Ghajar (2014) drift-flux model with previous scarce experimental and analytical studies for R12 and R134a flow with mass transfer occurred by pressure drop in adiabatic capillary tube. The liquid and vapor velocities of R134a calculated by the validated algorithm are set on the Yang and Shieh (2001) map to identify the possible flow pattern for each tube section.

3. PROBLEM FORMULATION

This study proposes to solve simultaneously the fundamental governing equations of fluid dynamics (continuity, energy and momentum equations) using drift flux model for refrigerant flow, which was divided into two different regions: a subcooled liquid monophasic flow and a saturated two-phase flow.

Some simplifying assumptions were made, such as: (i) steady-state, (ii) one-dimensional, (iii) isenthalpic flow, (iv) horizontal tube, (v) single tube of constant cross-sectional area, (vi) adiabatic flow, (vii) phase change without metastable effects, (viii) mechanical and thermal equilibrium between liquid-vapor mixture.

In the following, the necessary equations for calculating pressure drop, velocities and viscosity of liquid and vapor mixture are presented. All the variables nomenclature described in this document are reported in the section one.

3.1 Single phase liquid region equations

The flow in this region is incompressible, so the conservation of mass and linear momentum is given by Eq. (1) and Eq. (2), respectively.

$$\rho_L J_L A = c \tag{1}$$

$$\frac{\Delta P}{L} = -\frac{2C_f \rho_L J_L^2}{D} \tag{2}$$

3.2 Two-phase region - liquid and vapor equations:

In the drift flux model, the conservation equations are applied by considering the two-phase region as a mixture of liquid and vapor. Thus, the mixture formulae required to describe the studied flow is written below, Eqs. (3) to (5).

Conservation of mixture mass:

$$\frac{\partial}{\partial z}\left[G_G(z) + G_L(z)\right] = 0 \tag{3}$$

Conservation of mixture momentum:

$$\frac{\partial}{\partial z}\left[P(z) + \alpha(z)\rho_G(z)U_G{}^2(z) + (1-\alpha(z))\rho_L(z)U_L{}^2(z)\right] = -\overline{\tau_w}(z) \tag{4}$$

Conservation of mixture energy:

$$\frac{\partial}{\partial z}\left[G_G(z)\left(h_G(z)+\frac{U_G^2(z)}{2}\right)+G_L(z)\left(h_L(z)+\frac{U_L^2(z)}{2}\right)\right]=0 \tag{5}$$

The velocity of the vapor phase is defined by Zuber and Findlay (1965) drift-flux formulation, Eq. (6).

$$\frac{J_G}{\alpha}\equiv U_G = C_0 J_m + U_{Gm} \tag{6}$$

The distribution parameter, C_o, and the drift velocity, U_{Gm}, mentioned above, can be estimated through an independent flow pattern equation formulated by Bhagwat and Ghajar (2014), Eqs. from (7) to (11), who used 8255 experimental data points of two-phase flow for different conditions, such as air-water, air-kerosene, refrigerant fluids (R12, R22, R134a, R410a), pipe orientations (-90° to 90°), system pressure in a range of 0,1 – 18,1 MPa and hydraulic pipe diameters in a range of 0.5 to 305 mm. These authors also pointed out an observation, i.e., when liquid and vapor densities are equals, their model boils down to the homogeneous flow model.

$$C_0 = \frac{2\quad(\rho_G/\rho_L)^2}{1+(\mathrm{Re}_{tp}/1000)^2}+\frac{\left[\left(\sqrt{1+(\rho_G/\rho_L)^2/2}\right)^{(1-\alpha)}\right]^{2/5}+C_{0,1}}{1+(1000/\mathrm{Re}_{tp})^2} \tag{7}$$

$$C_{0,1}=\begin{cases}\left(0.2-0.2\sqrt{\rho_G/\rho_L}\right)\left[\left(2.6-\dfrac{J_G}{J_G+J_L}\right)^{0.15}-\sqrt{C_f}\right](1-x)^{1.5} & , Fr_{sv}>0.1\\ 0 & , Fr_{sv}\le 0.1\end{cases} \tag{8}$$

$$U_{Gm}=0.45\sqrt{\frac{gD(\rho_L-\rho_G)}{\rho_L}}(1-\alpha)^{0.5}C_2C_3 \tag{9}$$

$$C_2=\begin{cases}\left(\dfrac{0.434}{\log(\mu_{L,0})}\right)^{0.15} & , \quad \mu_{L,0}>10, \quad with \quad \mu_{L,0}=\dfrac{\mu_L}{0{,}001}\\ 1 & , \quad \mu_{L,0}\le 10\end{cases} \tag{10}$$

$$C_3=\begin{cases}(La/0.025)^{0.9} & , \quad La<0.025\\ 1 & , \quad La\ge 0.025\end{cases} \tag{11}$$

The dimensionless numbers described above are: Laplace variable, Froude number, mixture Reynolds number, Eqs.(12), (13) and (14), respectively.

$$La=\frac{1}{D}\sqrt{\frac{\sigma}{g(\rho_L-\rho_G)}} \tag{12}$$

$$Fr_{sg}=\sqrt{\frac{\rho_G}{(\rho_L-\rho_G)}}\frac{J_G}{\sqrt{gD}} \tag{13}$$

$$\mathrm{Re}_{tp}=\frac{J_m\rho_L D}{\mu_L} \tag{14}$$

The frictional pressure gradient of two-phase flow was determined from the homogeneous mixture hypothesis and two-phase multiplier model proposed by Friedel (1979). For both cases, the shear stress was calculated from Eq. (15) and Eq. (16), respectively.

$$\left(\frac{dp}{dz}\right)_{fric} = \bar{\tau}(z) = \frac{C_f \rho_m J_m^2}{2}\frac{S}{A} = \frac{2C_f \rho_m J_m^2}{D} \tag{15}$$

$$\frac{\left(\frac{dp}{dz}\right)_{fric}}{\left(\frac{dp}{dz}\right)_{fric,LO}} = \frac{\bar{\tau}(z)}{\left(\frac{dp}{dz}\right)_{fric,LO}} = (1-x)^2 + x^2\frac{\rho_L C_{f,GO}}{\rho_G C_{f,LO}} + \frac{3{,}24FH}{Fr^{0{,}045}We^{0{,}035}} \tag{16}$$

with *F*, *H*, *Fr*, *We* parameters calculated from Eqs. (17) to (20). The Fanning friction factor $C_{f,LO}$ and friction pressure drop $(dp/dz)_{fric,LO}$ are dependent on liquid properties, and $C_{f,GO}$ depends, only, on vapor properties.

$$F = x^{0,78}(1-x)^{0,224} \tag{17}$$

$$H = \left(\frac{\rho_L}{\rho_G}\right)^{0,91}\left(\frac{\mu_G}{\mu_L}\right)^{0,19}\left(1-\frac{\mu_G}{\mu_L}\right)^{0,7} \tag{18}$$

$$We = \frac{G_m{}^2 D}{\sigma\rho_m} \tag{19}$$

$$Fr = \frac{J_m^2}{gD} \tag{20}$$

The Fanning friction factor proposed by Haaland (1983), Eq. (21), was used in this study because all the conditions simulated are characterized by turbulent flow.

$$C_f = \left\{-3.6\log\left[\left(\frac{\varepsilon}{3.7D}\right)^{1.11} + \frac{6.9}{\mathrm{Re}}\right]\right\}^{-2} \tag{21}$$

Dukler et al. (1964) developed a similar expression to the density mixture (Ishii and Hibiki, 2010) for calculating the mixture viscosity, Eq. (22). Those equations are used in the mixture Reynolds determination, Eq. (23).

$$\psi_m = \alpha\psi_{G,Sat} + (1-\alpha)\psi_{L,Sat} \tag{22}$$

$$\mathrm{Re}_m = \frac{DJ_m\rho_m}{\mu_m} \tag{23}$$

4. SOLUTION METHODOLOGY

The solution algorithm was implemented in Fortran 90. This code allows the user to choose: the inlet pressure and temperature, tube characteristics, refrigerant fluid, whose thermophysic and thermodynamical properties were obtained by the Carnahan-Starling-DeSantis equation of state, and the phase velocities were determined by the drift-flux and homogeneous flow models. For homogeneous flow cases, the distribution parameter and the drift velocity were set to be unity and zero, respectively.

The momentum equation was solved applying an implicit fourth order Runge-Kutta (RK) algorithm. It was used a fixed integration step, which corresponds to the internal diameter for each tested case.

As the thermophysical properties are dependent with the pressure and the mixture stagnation enthalpy as well as the total mass flux are constant in any section of the capillary tube, the energy and mass equations were solved iteratively for each RK step through the implicit equation *f (p)*, Eq. (24), which solution was obtained by the secant method.

$$f(p) = p + G_V U_V + G_L U_L - \varpi \tag{24}$$

So, when the deviation of *f(p)* was reached in 10^{-1} Pa for the RK fourth step, the pressure, phase velocity, void fraction and quality were determined up to the end of the capillary tube. Figure 1 shows a simplified algorithm with the needed initial conditions and numerical integration procedures described above.

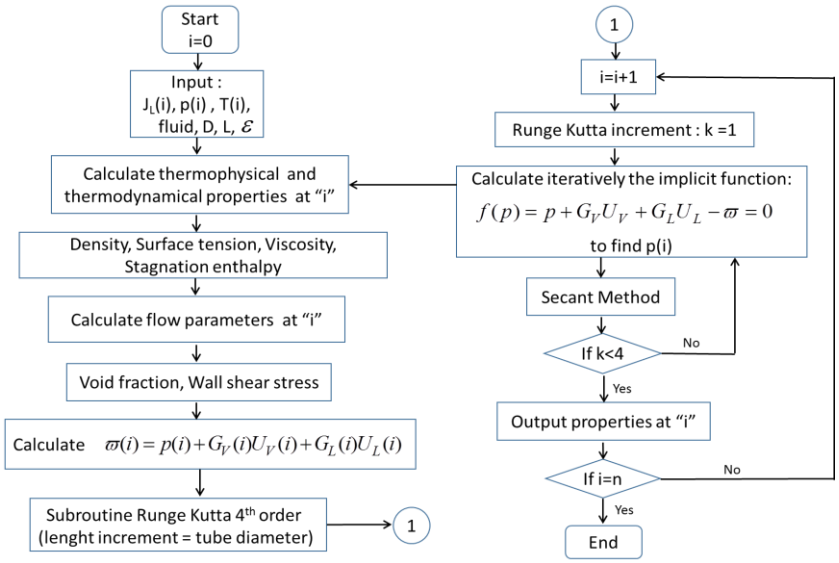

Figure 1. Flow chart of solving drift-flux model with mass transfer.

5. RESULTS AND DISCUSSION

The present approach was validated using experimental and simulated data available in the open literature. There were four different scenarios with liquid velocity, pressure and temperature inlet and geometrical capillary parameters, as shown in Tab. 1. For all cases, in the entrance, there is always only subcooled liquid flow. The simulations proposed considered that the two-phase flow comes up when the liquid pressure corresponds to the saturation pressure at the inlet temperature for the refrigerant fluid presented. So the metastable phenomenon reported by Lin et al. (1991) is not considered. For the scenarios analyzed, the distribution of: pressure, gas and liquid velocities, void fraction and quality along the capillary tube were calculated using drift-flux equation and the wall friction model and were used three setups: Bhagwat and Ghajar (2014) with homogeneous mixture model (BGH), Bhagwat and Ghajar (2014) with Friedel's correlation (BGF) and non-slip flow with wall friction based on homogeneous mixture hypothesis (HH).

Table 1. Inlet conditions for R12 and R134a in capillary tube.

Scenario	P (MPa)	J_L (m/s)	T(K)	D (mm)	ε (μm)	L (m)	Reference
#1	1.08	3.19	316	1.17	3.5	1.5	Lin et al. (1991)
#2	0.97	2.57	305	0.66	2.0	1.6	Li et al. (1990); Ingle et al. (2015)
#3	1.11	1.80	311	0.61	1.08	3.0	Melo et al.(1995); Seixlack et al.(2014)
#4	0.97	2.80	305	0.66	2.0	1.4	Liang and Wong (2001)

Figure 2 shows a comparative study between experimental data and numerical results using the three setups for the scenario #1. The quality along the tube length is shown in Fig. 2.b and the experimental data indicated a subcooled liquid flow until 0.5 m in contrast with 0.35 m obtained with all tested setups. This difference can be explained due to the R12 experimental vaporization didn't begin when the pressure was equal to the saturated pressure, so there was a metastable phenomenon as reported by Lin et al. (1991). In all numerical setups, the vaporization began when the pressure was equal to the saturation pressure at inlet temperature, which implied an early vaporization initiation. Regardless of this initial difference between experimental and simulated results, all setups show a similar qualitative behavior for quality distribution, especially the HH model, which is in better agreement with the measured data.

Figure 2.a shows a linear pressure drop with respect to the capillary length up to 0.35 m. This was the subcooled liquid flow region and the pressure variation is linear due to the wall friction (see Eq. (2)). After this point, the vaporization process began and the effect of flashing induced a non-linear pressure drop behavior. As a consequence, there was an increase in the quality and flow velocity. All three setups could capture the pressure behavior described above, but the BGF underestimated the pressure drop and BGH overestimated it. As a result of these, the quality was overestimated by BGH setup and underestimated by BGF. The best result for both pressure and quality as obtained by HH setup.

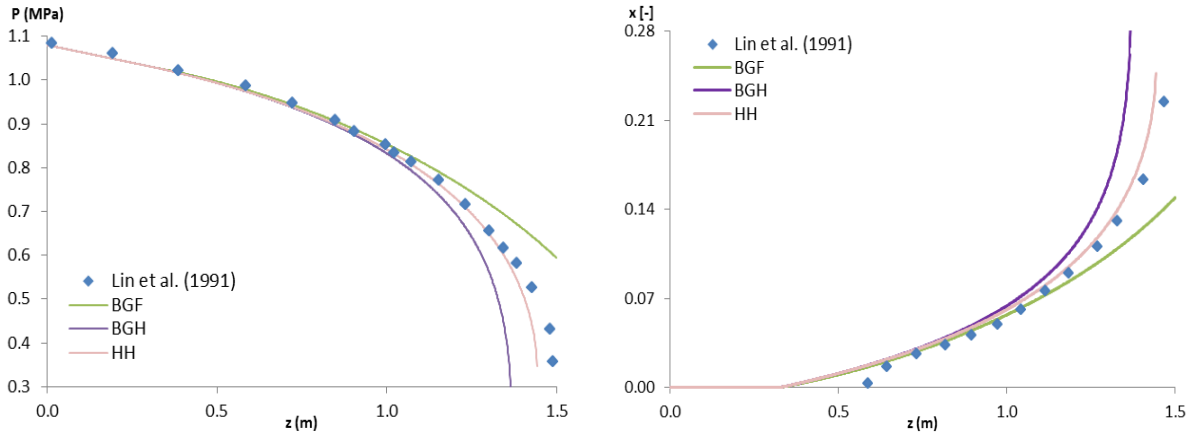

(a) (b)

Figure 2. (a) R12 experimental and calculated pressure drop for D=1.17 mm, (b) Distribution of quality.

Li et al. (1990) determined experimental data for the pressure drop of R12 flow. The results obtained by them were used for Ingle et al. (2015), who considered the homogeneous flow model and estimated the mass transfer by the cavitation model proposed by Zwart et al. (2004) as a constitutive relation for the volume fraction equation, Eq. (25).

$$\frac{\partial(\alpha_V \rho_V)}{\partial t} + \nabla.(\alpha_V \rho_V V_m) = F \frac{3\alpha_{nuc}(1-\alpha)\rho_v}{R_B}\sqrt{\frac{2|P_{sat}-P|}{3\rho_L}} \tag{25}$$

Figure 3 shows the results for all three numerical setups for the scenario #3 as well as Li et al. (1990) pressure drop experimental data and Ingle et al. (2015) void fraction distribution. Figure 3.a shows a reasonable agreement between all three simulation setups and pressure drop experimental data. The root mean squared (RMS) of the relative deviations was 1.5% for BGH, 0.9% for BGF and 2.3% for HH. Figure 3.b shows that the void fraction distribution matched well from 0.82 m, where represented the bubble point, up to 1.34 m.

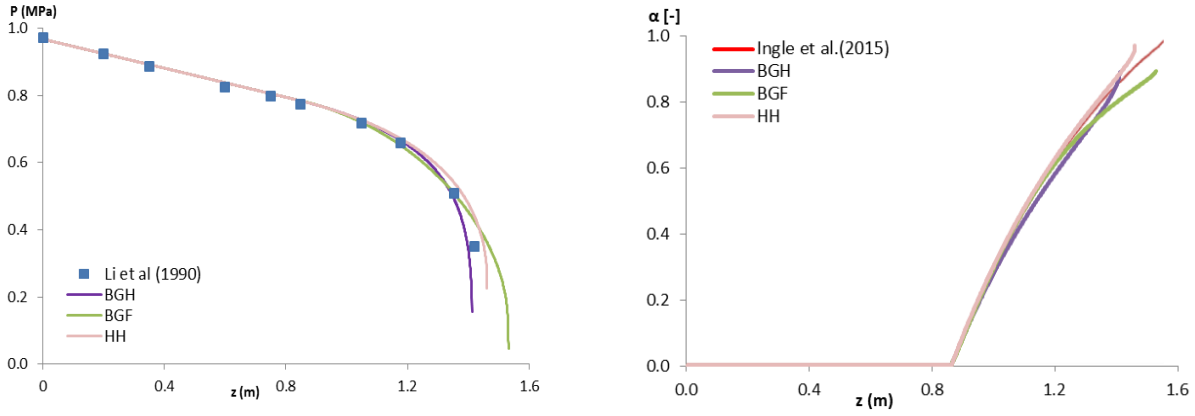

(a) (b)

Figure 3. (a) R12 experimental and calculated pressure drop for D=0.66 mm, (b) Distribution of void fraction.

Melo et al. (1995) determined the pressure profile for R134a by two ways, which are represented by "P_{ms}", measured pressure, and "P_{sat}", saturation pressure at the flow temperature. These data were used to validate the Seixlack et al. (2014) approach based on two-fluid model.

Figure 4.a shows that the results for the simulation using BGH were closer to the experimental data collected by Melo et al. (1995) than those obtained by Seixlack et al. (2014), which overestimated the pressure drop. As a consequence, Seixlack et al. (2014) reported higher void fraction and gas velocity along the capillary tube than any model studied, see Figs. 4.b and 4.c.

The pressure distribution obtained by the simulation considering BGF and HH were qualitatively similar, both decreased slowly even after the flashing point, but quantitatively distinct, 0.26 MPa/m and 0.18 MPa/m, respectively, which affected the gas velocity and mass quality, as shown in Figs. 4.b and 4.d.

Figure 4.c shows that the void fraction rised abruptly after the bubble point and approached to one near the end of the tube. The increase of quality is less pronounced in comparison to the void fraction, Fig. 4.d, due to the difference in the densities of the liquid and vapor phases.

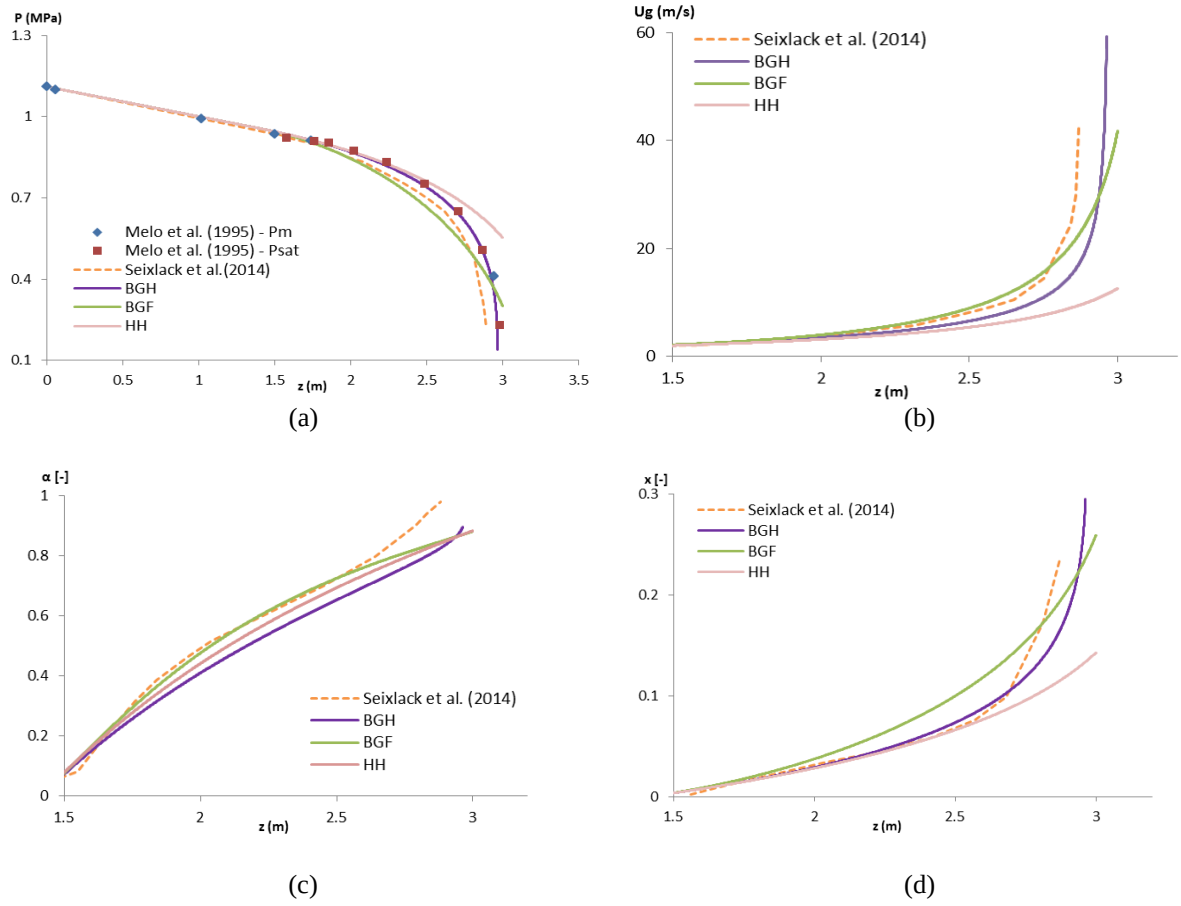

Figure 4. (a) R134a experimental and calculated pressure drop for D=0.61 mm, (b) Distribution of vapor velocity, (c) Distribution of void fraction, (d) Distribution of quality.

Figures 5.a up to 5.d show a comparison of phase velocities, pressure drop and void fraction between the simulated cases and the results obtained by Liang and Wong (2001), who used the correlation presented by Zuber and Findlay (1965) for drift velocity relative to the center of the mass of the mixture estimation, Eq. (26).

$$\frac{dU_{Gm}}{dz} = \frac{d}{dz}\left\{1.48\frac{\rho_L}{\rho_m}\left[\frac{(\rho_L - \rho_g)g\sigma}{\rho_L{}^2}\right]\right\} \tag{26}$$

Figure 5.a shows a good concordance between Liang and Wong (2001) analytical study and the results of this work for HH setup. Results using BGF presented larger deviations for z >1.19 m. This pressure drop discrepancy affected the achieved values of void fraction and velocities of gas and mixture, as shown in Figs. 5.b, 5.c and 5.d by green lines. The simulation performed with BGH overestimated the pressure drop mainly for distances greater than 1.1 m, where the concavity of purple line in Fig. 5.b changes and the void fraction and gas velocity increased sharply, see Fig. 5.d. Once liquid phase continuously flashed into vapor due to the frictional force, the ρ_G/ρ_L ratio was less than unity and in order to remain the total mass flux constant in the whole length of the duct, the velocity of vapor phase needed to increase fast. In the two-phase flow region, the mixture velocity increased due to the high void fraction values and the decreased in the mixture density.

Besides, the mixture velocity approached the vapor velocity near the exit of the tube, see Figs. 5.c and 5.d, where the void fraction was greater than 0.8. In Fig. 5.b, one can see a delay in vapor generation for the simulation proposed in comparison of Liang and Wong (2001) results. A careful analysis shows that the referred authors' calculations of pressure drop for monophasic flow, 0<z<0.6 m, was a slightly bigger than one estimated by this study, 0<z< 0.65 m.

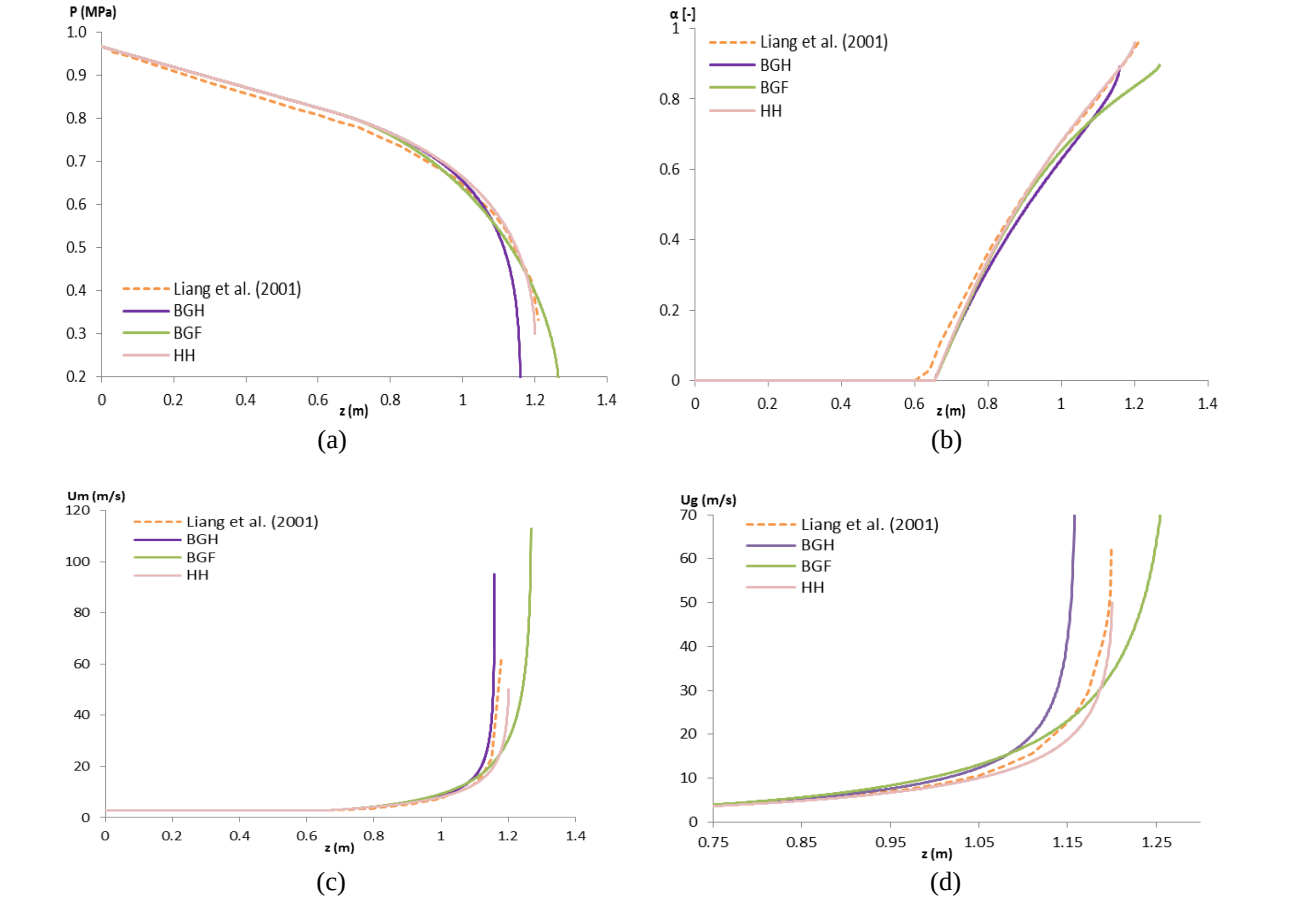

Figure 5. (a) R134a pressure drop calculated for D=0.66 mm, (b) Distribution of void fraction, (c) Distribution of mixture velocity, (d) Distribution of vapor velocity.

Yang and Shieh (2001) provides a R134a two-phase flow pattern investigation and mentioned that is no flow pattern model able to well predict the behavior of refrigerant flow in small diameter tube. So, the results of the Fig. 6 shows the possible flow patterns observed in a vertical pipe with length of 30 m, 2 mm ID, 1.08 µm roughness and 800 kg/m².s mass flux of R134a, with 303 K inlet temperature and 0.775 MPa initial pressure.

Figure 6 shows that the flow pattern may change according to the generation of vapor phase. Besides, the highest pressure drop, 68 kPa/m, occurred in annular flow section, which is explained by the abrupt change in quality from 0.09 to 0.35.

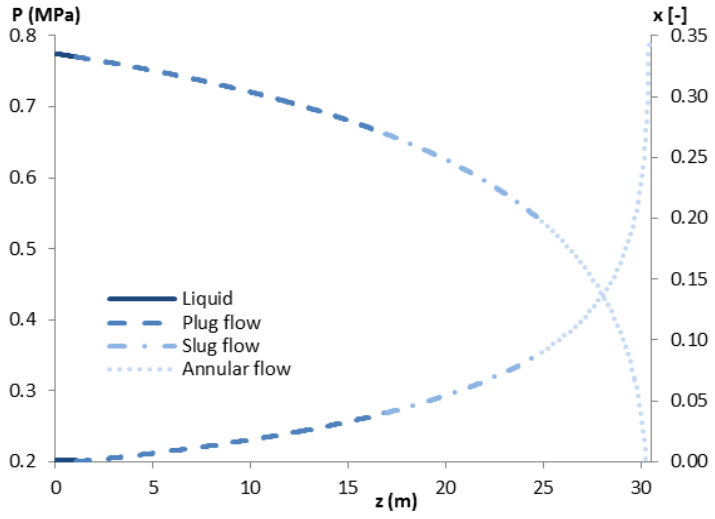

Figure 6. Two-phase flow patterns in capillary tube of D=2mm.

6. CONCLUSIONS

A flow pattern independent void fraction correlation developed by Bhagwat and Ghajar (2014) with homogenous wall shear stress models was used for modeling the mass transfer mechanism caused by pressure drop of refrigerant two-phase flow through adiabatic capillary tube. The results showed that this approach predicted well the flow parameters in comparison with the existing experimental data available in the literature and results obtained by two-fluid model, which reveals a strong point of this formulation, once the studied approach goes without interfacial properties and the knowledge of the phases distribution. Also, with a use of a reliable flow pattern map in terms of effect of tube size and fluid properties, it is possible to predict a particular type of geometric distribution of the vapor and liquid phases.

7. ACKNOWLEDGEMENTS

The authors wish to acknowledge the financial support of the PETROBRAS.

8. REFERENCES

Arcanjo, A.A., Tibiriçá, C.B., Ribatski, G., 2010. “Evaluation of flow patterns and elongated bubble characteristics during the flow boiling of halocarbon refrigerants in a micro-scale channel”. Experimental Thermal and Fluid Science, Vol. 34, pp. 766-775.

Bhagwat, S.M. and Ghajar, A. J., 2014. “A flow pattern independent drift flux model based void fraction correlation for a wide range of gas-liquid two phase flow”. International Journal of Multiphase Flow, Vol. 59, pp. 186-205.

Chisholm, D., 1973. “Void fraction during two-phase flow”. Journal of Mechanical Engineering Science, Vol. 15, pp. 235-236.

Dukler, A.E., Wicks, M., Cleveland, R.G., 1964. “Frictional pressure drop in 2-phase flow: B. an approach through similarity analysis”. AIChE Journal, Vol. 10, No. 1, pp. 44-51.

Friedel, L., 1979. “Improved friction pressure drop correlations for horizontal and vertical two-phase pipe flow”. European two-phase flow group meeting, Ispra, Italy, pp. 485-492. Paper E2.

Haaland, S. E., 1983. “Simple and explicit formulas for the friction fator in turbulent pipe flow”. Journal of Fluids Engineering, Vol.105, No. 1, pp. 89-90.

Ingle, R., Rao, V.S., Mohan, L.S.; Dai, Y., 2015. “Modelling of flashing in capillary tubes using homogeneous equilibrium approach”. Procedia IUTAM Symposium on Multiphase Flows with Phase Change: Challenges and Opportunities, Vol. 15, pp. 286-292.

Ishii, M. and Hibiki, T., 2010. Thermo-Fluid Dynamics of Two-Phase Flow. Springer, New York.

Li, R.Y., Lin, S., Chen, Z.H., 1990. “Numerical modelling of thermodynamic non-equilibrium flow of refrigerant through capillary tubes”, ASHRAE Transactions, Vol. 96, Part 1, pp.542-549.

Liang, S.M. and Wong, T.N., 2001. “Numerical modeling of two-phase refrigerant flow through adiabatic capillary tubes”. Applied Thermal Engineering, Vol. 21, No. 10, pp. 1035-1048.

Lin, S., Kwok, C.C.K., Li, R.Y, Chen, Z.H., Chen, Z.Y., 1991. “Local frictional pressure drop during vaporization of R-12 through capillary tubes”. International Journal of Multiphase Flow, Vol. 17, No. 1, pp. 95-102.

Madsen, N., 1975. "A void fraction correlation for vertical and horizontal bulk-boiling of water”. AIChE Journal, Vol. 21, pp. 607-608.

Melo, C.; Ferreira, R.T.S.; Boabaid, N.C.; Gonçalves, J.M., 1995. “Experimentation and analysis of refrigerante flow through adiabatic capillary tubes”. In Proceedings of the ASME 1995 International Mechanical Engineering Congress and Exposition, pp. 19-30.

Mezavila, M. M., 1995. Simulação do escoamento de fluidos refrigerantes em tubos capilares não-adiabáticos. M.S. dissertation, Universidade Federal de Santa Catarina, Florianópolis, SC, Brazil.

Seixlack, A. L., Prata, A. T., Melo, C., 2014. “A two-fluid model for refrigerant flow through adiabatic capillary tubes”. Journal of the Brazilian Society of Mechanical Sciences and Engineering, Vol. 36, No. 1, pp. 1-12.

Wallis, G. B., 1980. “Critical two-phase flow”. International Journal of Multiphase Flow, Vol. 6, pp. 97-112.

Yang, C. Y., Shieh, C. C., 2001. “Flow pattern of air-water and two-phase R-134ª in small circular tubes”. International Journal of Multiphase Flow, Vol. 27, pp. 1163-1177.

Zuber, N. and Findlay, J., 1965. “Average volume concentration in two phase systems”. Journal of Heat Transfer, Vol. 87, No. 4, pp. 453-468.

Zwart, J., Gerber A. G., Belamri, T., 2004. “Two-Phase Flow Model for Predicting Cavitation Dynamics”. In Proceedings of the 5th International Conference on Multiphase Flow, Yokohama, Japan. Paper no. 152.

9. RESPONSIBILITY NOTICE

The authors are the only responsible for the printed material included in this paper.